Cross Sections and Transverse Single-Spin Asymmetries in Forward Jet Production from Proton Collisions at $\sqrt{s} = 500\,\mathrm{GeV}$

L. C. Bland,[1] E. J. Brash,[2] H. J. Crawford,[3] A.A. Derevschikov,[4] K. A. Drees,[1] J. Engelage,[3] C. Folz,[1] M. K. Jones,[5] E. G. Judd,[3] X. Li,[6,1] N. K. Liyanage,[7] Y. Makdisi,[1] N. G. Minaev,[4] R. N. Munroe,[2] L. Nogach,[4] A. Ogawa,[1] C. F. Perdrisat,[8] C. Perkins,[3] M. Planinic,[9] V. Punjabi,[10] G. Schnell,[11,12] G. Simatovic,[9,1] T. G. Throwe,[1] C. Van Hulse,[11] and A. N. Vasiliev[4]

(A_NDY Collaboration)[*]

[1] *Brookhaven National Laboratory, Upton, New York 11973, USA*
[2] *Christopher Newport University, Newport News, Virginia 23606, USA*
[3] *University of California, Berkeley, California 94720, USA*
[4] *Institute of High Energy Physics, Protvino 142281, Russia*
[5] *Thomas Jefferson National Accelerator Facility, Newport News, Virginia 23606, USA*
[6] *Shandong University, Jinan, Shandong 250100, China*
[7] *University of Virginia, Charlottesville, Virginia 22903, USA*
[8] *College of William and Mary, Williamsburg, Virginia 23187, USA*
[9] *University of Zagreb, Zagreb, HR-10002, Croatia*
[10] *Norfolk State University, Norfolk, Virginia 23504, USA*
[11] *Department of Theoretical Physics, University of the Basque Country UPV/EHU, 48080 Bilbao, Spain*
[12] *IKERBASQUE, Basque Foundation for Science, 48011 Bilbao, Spain*

(Dated: April 5, 2013)

Measurements of the production of forward jets from polarized proton collisions at $\sqrt{s} = 500\,\mathrm{GeV}$ are reported. Our measured jet cross section is consistent with hard scattering expectations. Our measured analyzing power for forward jet production is small and positive, consistent with the existence of partonic orbital angular momentum.

PACS numbers: 12.38.Qk,13.87-a,13.88+e

The proton is a building block of matter, which is itself built from elementary quarks (q) and gluons (g). Our understanding of the structure of the proton has become increasingly sophisticated since the advent of Quantum Chromodynamics (QCD), and a reason for this has been the quest to understand how the proton gets its intrinsic spin from its constituents. The present view is that q or g orbital angular momentum (OAM) makes important contributions to the proton spin. Early indications of this came from large analyzing powers (A_N) measured in the production of charged and neutral pions in collisions of transversely polarized protons at center-of-mass energy $\sqrt{s} = 20\,\mathrm{GeV}$ [1]. A_N is the amplitude of the spin-correlated azimuthal modulation of the produced particles. A large A_N is not expected for pions produced with sufficient transverse momentum (p_T) in collinear perturbative QCD (pQCD) at leading twist, due to the chiral properties of the theory [2]. Measurements of large A_N for π production at large Feynman-x ($x_F = 2p_z/\sqrt{s}$) prompted theorists to introduce spin-correlated transverse momentum (k_T) in either the initial state (Sivers effect [3]) or the final state (Collins effect [4]). For inclusive π production, these effects cannot be disentangled. In contrast, in measurements of jets, defined as a collimated multiplicity of energetic baryons and mesons that are produced in high-energy collisions, contributions from fragmentation are absent and hence information about the scattered q or g can be inferred directly. In particular, A_N for jet production, direct photons or Drell-Yan processes is expected to arise only from the Sivers effect. The initial-state spin-correlated k_T is related by models [5] to q and g OAM.

Large A_N for π production at large x_F in $p^\uparrow + p$ collisions at $\sqrt{s} \leq 20$ GeV [1, 6] have challenged understanding, because cross sections are much larger than pQCD expectations, resulting in skepticism that π production in these kinematics is from hard-scattering processes. Theoretical interest in understanding A_N for π production has been revived by recent measurements [7, 8] at $\sqrt{s} \geq 62$ GeV, where cross sections [9] are in agreement with pQCD. Furthermore, measurements of A_N for π production in $p^\uparrow + p$ collisions at $\sqrt{s} \geq 62$ GeV have been concurrent with measurements of transverse single-spin asymmetries (SSA) in semi-inclusive deep inelastic scattering (SIDIS) [10], where an electron or muon is inelastically scattered from a proton, whose spin is transverse to the lepton beam. Meson fragments of the struck q are found to have spin-correlated azimuthal modulations, whose amplitudes are understood by the Sivers and Collins effects, introduced to explain A_N for $p^\uparrow + p \to \pi + X$. An alternative and complementary theoretical approach based on collinear factorization [11] predicts A_N involving twist-3 multi-parton correlations [12], and is expected to be related to the Sivers and Collins functions via transverse-momentum moments. However, an attempt at linking the different approaches using data

from SIDIS and $p^\uparrow + p \to \pi + X$ yielded a mismatch in the sign [13]. Thus a consistent understanding of all transverse SSA in hard scattering processes is not yet within our grasp, but would greatly benefit from measurements of A_N for jet production in $p^\uparrow + p$ collisions, since it receives no contributions from the Collins effect.

In this Letter, we report first measurements of cross sections and A_N for forward jet production in $p^\uparrow + p$ collisions at $\sqrt{s}$=500 GeV. The measurement was conducted with the A$_N$DY detector at the 2 o'clock interaction region (IP2) of the Relativistic Heavy Ion Collider (RHIC) at Brookhaven National Laboratory. The primary detector components were two mirror-symmetric hadron calorimeter (HCal) modules that were mounted to face one of the beams at IP2 for the 2011 and 2012 RHIC runs, and spanned the pseudorapidity interval $2.4 < \eta < 4.0$ that is well shielded from single beam backgrounds by the cryostats of the ring magnets.

Each HCal consisted of a 12-row × 9-column matrix of (10 cm)^2 × 117 cm lead cells, each with an embedded 47 × 47 matrix of scintillating fibers [14]. For the 2012 run, two 5-row × 2-column arrays were deployed above and below the beams to create an annular HCal with a central 20×20 cm^2 hole for the beams. The HCal positions were measured by survey. The A$_N$DY apparatus also had a pair of 16-element scintillator annuli mounted symmetrically about IP2 to serve as a beam-beam counter (BBC) [15], a pair of 7-row×7-column lead glass detector arrays serving as small electromagnetic calorimeters (ECal) at a fixed (variable) position for the 2011 (2012) run, a scintillator preshower array and a pair of zero-degree calorimeter (ZDC) modules [17] that faced each beam. A GEANT [16] model of A$_N$DY was created, as described in Ref. [18], and uses inputs from PYTHIA 6.222 [19], hereafter referred to as full simulation.

$p^\uparrow + p$ collisions were initiated at IP2 at systematically different times in stores during the 2011 run to assess the impact of a third collision point on operations. The colliding beam luminosity at IP2 was measured by the vernier scan technique and resulted in σ=0.94±0.08 mb for the effective cross section of coincidences between the ZDC modules which were used to continuously monitor the luminosity. Results reported here were from 6.5 pb^{-1} of integrated luminosity during the 2011 run at $\sqrt{s}$=500 GeV and 2.5 pb^{-1} of integrated luminosity during the 2012 run at $\sqrt{s}$ = 510 GeV. The polarization of each beam was measured by a relative polarimeter at several times in each fill. The relative polarimeter was calibrated from measurements from an absolute polarimeter, resulting in 0.526±0.027 (0.511±0.028) [20] for the average beam polarization for our jets at $x_F > 0$ ($x_F < 0$) in the 2011 run.

The data by A$_N$DY is from 32-channel 70 MHz flash analog-to-digital (ADC) converters with 0.25 pC/count sensitivity and noise levels < 0.25 pC. Online pedestal corrections were made on board by field-programmable gate arrays (FPGA). Pedestal-corrected ADC counts were then analyzed by the FPGA to derive an event trigger. The majority of the data were from our jet trigger that summed the ADC response from each HCal module, excluding the outer two perimeters of cells. This trigger is sensitive to electromagnetic (EM) and charged hadron fragments of jets. Events were also acquired from a minimum-bias trigger that required minimum charge from any element of the annular BBC that faced each beam, sometimes with a collision vertex requirement, where the vertex is reconstructed by the FPGA from time-difference measurements. Some events were acquired when either ZDC crossed threshold as a way to tune bunch-crossing scalers used to monitor luminosity and the polarization of colliding beams.

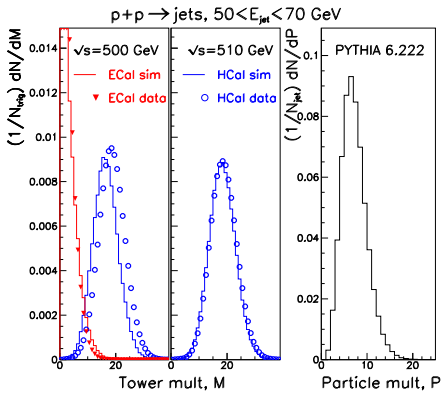

FIG. 1: Tower multiplicity distributions for forward jets for data compared to full simulations for (left) jets from $\sqrt{s}$=500 GeV collisions, as used for the jet analyzing power; and for (middle) jets from $\sqrt{s}$=510 GeV collisions, as used for the jet cross section. (Right) Multiplicity of particles produced by PYTHIA 6.222 [19] that gives rise to the forward jet.

The HCal had individual cell gains adjusted prior to colliding beam operation based on their cosmic-ray muon responses. The first step in the offline analysis was to determine the absolute energy scale of the HCal modules by reconstruction of $\pi^0 \to \gamma\gamma$ from pairs of single-cell clusters, that had neighboring cells with energy $E' < 0.11$ GeV, where E' is the incident photon equivalent energy. The π^0 identification was confirmed by associating the single-cell clusters reconstructed from our full simulations with primary photons generated by PYTHIA [18]. Offline analysis also refined the relative calibration of all cells by a combination of π^0 reconstruction and the matching of energy-deposition distributions from single cells between data and full simulation. For the jet analyses described below, the energy calibration was adjusted to account for the average difference between hadronic and EM showers from full simulations. We used $E = 1.12 \times E' - 0.1$ GeV, where E is the equivalent incident energy measured by individual cells as used in the jet finders and E' is from π^0 calibration.

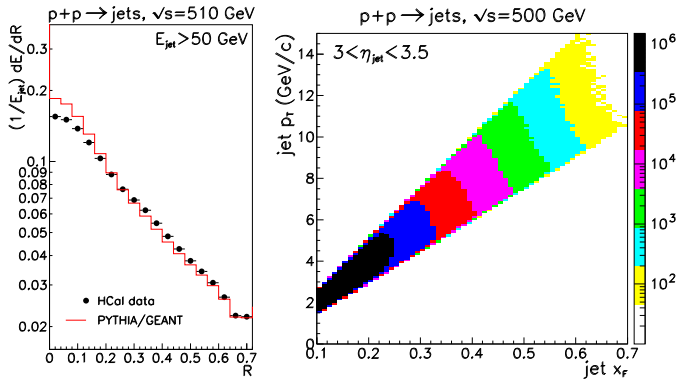

FIG. 2: (left) Event averaged jet shape, corresponding to how the energy depends on R, the distance a tower is from the thrust axis in (η, ϕ) space. (right) Correlation between jet x_F and p_T.

Our final jet results use the anti-k_T jet algorithm [21] with a cone radius of R_{jet}=0.7 radians in (η, ϕ) space, although we have also considered cone algorithms [22]. For each event, the η_i, ϕ_i of each cell with $E > E_{thr}$ (E_{thr} = 0.25 GeV is used to make towers) is reconstructed from its surveyed position and the z position of the collision vertex for the event, calculated from the measured time difference between the two BBC annuli. The anti-k_T algorithm reconstructs the jet by a pair-wise merging of tower clusters separated by $d_{ij} = \min(k_{T,i}^{-2}, k_{T,j}^{-2}) \times (R_{ij}^2/R_{jet}^2)$, when $d_{ij} < 1/k_{T,i}^2$ for any i. Each tower has a transverse momentum $k_{T,i} = E_i/\cosh(\eta_i)$, assuming zero mass for the incident particle. Pairs of tower clusters are separated by $R_{ij} = \sqrt{(\eta_i - \eta_j)^2 + (\phi_i - \phi_j)^2}$. The merging procedure is repeated until all towers are accounted for. A valid jet is considered to have $|\eta_{jet} - \eta_0| < d\eta$ and $|\phi_{jet} - \phi_0| < d\phi$, where $\eta_{jet}(\phi_{jet})$ are computed from the energy-weighted averages of towers included in the jet within the acceptance centered at η_0, ϕ_0 of half-width dη, dϕ. For the 2011 data, both ECal and HCal cells were considered. For the 2012 data with ECal positioned beyond the HCal acceptance, only HCal cells are considered. Our cross section and analyzing power results are reported using η_0=3.25, dη=0.25 and dϕ=0.5. The HCal module to the left (right) of the oncoming beam has $\phi_0 = 0\,(\pi)$.

The tower multiplicity distributions for valid jets are shown in Fig. 1. This figure compares jets reconstructed from data to jets reconstructed from our full simulations of p+p collisions, where the GEANT response uses the individual cell calibrations to produce simulated ADC values, and the jet trigger is emulated by the same algorithm used by the FPGA for our measurements. In general, the simulation gives an excellent description of the data, consistent with minimal contributions from single-beam backgrounds, as determined from direct measurement, or from other unknown sources of energy deposition (underlying event). Small increases in the HCal multiplicity for 2011 are attributed to ancilliary material (e.g., cables, etc.) not included in GEANT, prompting us to use the 2012 data for the jet cross section. The reconstructed jets have a broad tower multiplicity distribution whose mean value increases as E_{jet} increases. Given that data and full simulation agree, we can then infer the distribution of particles in the jet by applying the anti-k_T jet finder to detectable particles produced by PYTHIA. These particle jets have similar multiplicity to those reconstructed in e^+e^- collisions at $\sqrt{s} \approx 10$ GeV [23] and in fixed-target hadroproduction experiments [25]. Such low multiplicity jets are generally not accessible in hadron colliders because their p_T is too low. Forward detection results in large x_F, so makes their detection possible.

The towers included in the jets have their energy distributed relative to the thrust axis in a manner that is typical of a jet (Fig. 2). Most of the energy is concentrated near the thrust axis. As towers become increasingly distant from the thrust axis, on average they contribute little to the energy of the jet. The data is well described by our full simulation, although there are some indications that jets produced by PYTHIA 6.222 [19] have energy concentrated closer to the thrust axis relative to our measurements. Also shown in Fig. 2 is the correlation between x_F and p_T for our jet events. The dη requirement strongly correlates these two kinematic variables.

The jet energy scale was established by comparing tower jets reconstructed from the full simulation to particle jets reconstructed from PYTHIA, and resulted in the hadronic compensation described earlier. A check of the energy scale was made for 3-jet events in the data by the centroid of a peak attributed to $\Upsilon(1S) \rightarrow 3g$ [23]. This peak has statistical significance of 3.5σ. The centroid of the peak depends smoothly on R_{jet} used in the anti-k_T algorithm, as do our measures of the jet-energy scale from simulation.

The forward jet production cross section was measured by scaling the number of reconstructed jets by the measured integrated luminosity and correction factors described here. For jet triggers, there is a trigger efficiency (ϵ_{trig}) dominated by the variation of η along the collision vertex distribution. ϵ_{trig} is evaluated as a function of jet energy from the full simulation, and is checked by comparing invariant jet cross sections from jet-triggered events to cross sections determined from the minimum-bias trigger. The jet detection efficiency (ϵ_{jet}) is determined from the ratio of number of tower jets within the acceptance to the number of particle jets within the acceptance. ϵ_{jet} is checked by systematically varying the acceptance and assessing the stability of the resulting invariant cross section. Sources of systematic uncertainty are (a) values of ϵ_{trig} and ϵ_{det}; (b) time-dependent effects from either HCal gain stability or from beam conditions; (c) jet-energy scale uncertainties; (d) luminosity normal-

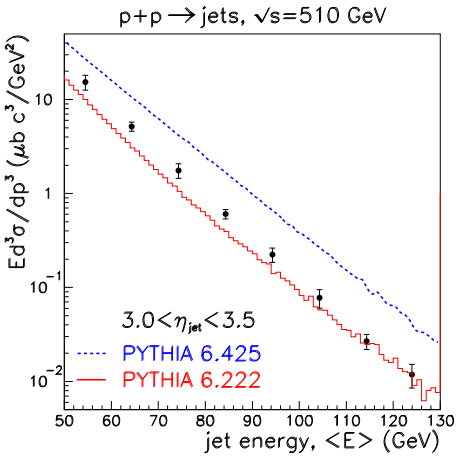

FIG. 3: Invariant forward jet cross section measured at $\eta = 3.25$. Our measurements are compared to predictions by PYTHIA.

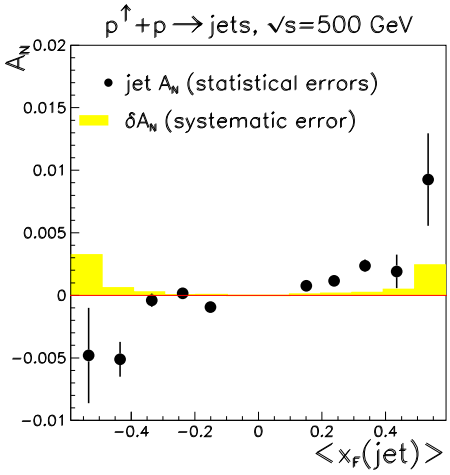

FIG. 4: Analyzing power for forward jet production. Jets are reconstructed with the anti-k_T algorithm using $R_{jet} = 0.7$. Preliminary results [22] reported comparable A_N with the mid-point cone algorithm. Systematic error estimates are described in the text, and do not include scale uncertainty from the beam polarization measurements.

ization; and (e) jet-finder parameters (R_{jet}, E_{thr}) that also probe underlying event contributions. The resulting distribution of forward jet cross section as a function of energy is shown in Fig. 3. Our results are compared to PYTHIA 6.222 [19] and 6.425 [24] predictions for anti-k_T jets reconstructed from stable particles that are within the detector acceptance. In Ref. [22] it was shown that PYTHIA predicts forward jets are from partonic hard scattering. PYTHIA 6.222 is prior to tunings based on Tevatron data which resulted in later versions (e.g., 6.425) used by the LHC. Versions of PYTHIA that predate tunings for the LHC are known to accurately describe large x_F π^0 production [26], and are known to lose accuracy for more complicated multi-particle correlations [27].

The forward jet A_N is measured by the cross-ratio method, that cancels through second order luminosity and detector asymmetries by combining spin up ($\uparrow$) and spin down ($\downarrow$) measurements from nominally mirror symmetric beam-left (L) and beam-right (R) hadron calorimeter modules. The jet analyzing power is

$$A_N = \frac{1}{P_{beam}} \frac{\sqrt{N_L^{\uparrow} N_R^{\downarrow}} - \sqrt{N_L^{\downarrow} N_R^{\uparrow}}}{\sqrt{N_L^{\uparrow} N_R^{\downarrow}} + \sqrt{N_L^{\downarrow} N_R^{\uparrow}}}. \qquad (1)$$

Each fill has a pattern of spin directions for bunches of beam injected into RHIC. A specific crossing of bunches from the two rings is the remainder after dividing the RHIC clock count for an event by 120. The bunch-crossing distribution has characteristic holes that correspond to missing bunches from one or the other beam. The pattern of polarization directions for that fill recorded at A$_N$DY originating from information broadcast by RHIC, is then used to accumulate $N_{L(R)}^{\uparrow(\downarrow)}$ in the analysis. Since the RHIC broadcast information specifies polarization directions at the polarized ion source, we rely on the measurement of spin asymmetries for far-forward neutron production measured by the ZDC, where the A_N was previously measured [28], to ensure the jet A_N is measured with the proper sign.

Our measured forward jet A_N is shown in Fig. 4. One check for systematic effects was to fit the spin asymmetry ($\epsilon = P_{beam} A_N$) measured in each jet $\langle x_F \rangle$ bin for each RHIC fill by a constant. The resulting χ^2 per degree of freedom from these fits is close to unity, and is consistent with the statistical errors, meaning the systematic errors are small. A more quantitative check for systematic effects was to establish if an effectively unpolarized sample of $p+p$ collisions had A_N consistent with zero. This was accomplished by a random reversal of the spin direction for half of the filled bunch crossings. The mean value of ϵ for $\sim$ 100 random spin direction patterns had values $10^{-5} < \epsilon < 10^{-4}$ resulting in the systematic uncertainty estimate of 2×10^{-4} for the jet A_N. The systematic error estimates in Fig. 4 are estimated by varying the jet finder and valid jet parameters. Our jet A_N measurement is limited by statistics. Our measured small and positive jet A_N is naively expected because $A_N(\pi^+) \approx -A_N(\pi^-)$, thus giving cancelling contributions from $\pi^{\pm}$ in a jet.

In conclusion, we have made first measurements of forward jet production in $p^{\uparrow} + p$ collisions at $\sqrt{s}$=500 GeV. Our measured cross section is consistent with dominant contributions from partonic hard scattering, even though the transverse momentum for the produced jets is small ($2 < p_T < 10$ GeV/c). We have measured the analyzing power for forward jet production, and find it to be small and positive. Our measurements constrain knowledge [29] of Sivers functions, that are related to parton

OAM through models. It remains the case that the most definitive experiment to test present understanding is a measurement of the analyzing power for DY production.

We thank the RHIC Operations Group at BNL. This work was supported in part by the Office of NP within the U.S. DOE Office of Science, the Ministry of Ed. and Sci. of the Russian Federation and the Ministry of Sci., Ed. and Sports of the Rep.of Croatia, and IKERBASQUE and the UPV/EHU under program UFI 11/55.

* URL: `www.andy.bnl.gov`

[1] B. E. Bonner *et al.*, Phys. Rev. Lett. **61**, 1918 (1988); D. L. Adams *et al.*, Phys. Lett. B **261**, 201 (1991);**264**, 462 (1991).

[2] G. L. Kane, J. Pumplin, W. Repko, Phys. Rev. Lett. **41**, 1689 (1978).

[3] D. Sivers, Phys. Rev. D **41**, 83 (1990); **43**, 261 (1991).

[4] J. Collins, Nucl. Phys. B **396**, 161 (1993).

[5] M. Burkardt, G. Schnell, Phys. Rev. D **74**, 013002 (2006).

[6] R. D. Klem *et al.*, Phys. Rev. Lett. **36**, 929 (1976); W. H. Dragoset *et al.*, Phys. Rev. D **18**, 3939 (1978); B. E. Bonner *et al.*, Phys. Rev. D **41**, 13 (1990); C. E. Allgower *et al.*, Phys. Rev. D **65**, 092008 (2002).

[7] J. Adams *et al.*, Phys. Rev. Lett. **92**, 171801 (2004).

[8] I. Arsene *et al.*, Phys. Rev. Lett. **101**, 042001 (2008).

[9] J. Adams *et al.*, Phys. Rev. Lett. **97**, 152302 (2006).

[10] A. Airapetian *et al.* (HERMES), Phys. Rev. Lett. **103**, 152002 (2009); **94**, 012002 (2005); C. Adolph *et al.* (COMPASS), Phys. Lett. B **717**, 376 (2012); **717**, 383 (2012).

[11] A. V. Efremov and O. V. Teryaev, Sov. J. Nucl. Phys. **36**, 140 (1982) [Yad. Fiz. **36**, 242 (1982)]; Phys. Lett. B **150**, 383 (1985); J.-Qiu and G. F. Sterman, Phys. Rev. Lett. **67**, 2264 (1991); Nucl. Phys. B **378**, 52 (1992); Phys. Rev. D **59**, 014004 (1998).

[12] Y. Koike, Nucl. Phys. A **721**, 364c (2003); C. Kouvaris *et al.*, Phys. Rev. D **74**, 114013 (2006);

[13] Z.-B. Kang *et al.*, Phys. Rev. D **83**, 094001 (2011).

[14] T. A. Armstrong *et al.*, Nucl. Instrum. Meth. A **496**, 227 (1998).

[15] R. Bindel, E. Garcia, A. C. Mignerey, L. P. Remsberg, Nucl. Instrum. Meth. A **474**, 38 (2001).

[16] GEANT 3.21, CERN program library.

[17] C. Adler, A. Denisov, E. Garcia, M. Murray, H. Strobele, S. White, Nucl. Instrum. Meth. A **499**, 433 (2003).

[18] C. Perkins, *XIX International Workshop on Deep-Inelastic Scattering*, Newport News (2011) [arXiv:1109.0650].

[19] T. Sjöstrand *et al.*, Computer Physics Commun. **135**, 238 (2001).

[20] Polarimetry Group, *RHIC polarization for runs 9-12*, https://wiki.bnl.gov/rhicspin/upload/6/68/Run91112_results.pdf (2012).

[21] M. Cacciari, G. P. Salam, G. Soyez, JHEP **0804**, 063 (2008).

[22] L. Nogach (for A_NDY), *20^{th} International Symposium on Spin Physics* (2012) [arXiv:1212.3437].

[23] M. S. Alam *et al.* (CLEO), Phys. Rev. D **56**, 17 (1997).

[24] T. Sjöstrand, S. Mrenna, P. Skands, JHEP **05**, 026 (2006).

[25] C. Bromberg *et al.*, Phys. Rev. Lett. **38**, 1447 (1977); M. .D. Corcoran *et al.*, Phys. Rev. Lett. **41**, 9 (1978); **44**, 514 (1980); M. W. Arenton *et al.*, Phys. Rev. D **31**, 984 (1985).

[26] L. C. Bland (for STAR), *X^{th} Advanced Research Workshop on High Energy Spin Physics*, (2003) [hep-ex/0403012].

[27] A. Gordon (for STAR), *Recontres de Moriond QCD and High Energy Interactions* (2009) [arXiv:0906.2332].

[28] Y. Fukao *et al.*, Phys. Lett. B **650**, 325 (2007).

[29] L. Gamberg, Z. B. Kang, A. Prokudin, submitted to Phys. Rev. Lett. [arXiv:1302.3218].